

Vibrational spectroscopic study on trigonal polyoxymethylene and polyoxymethylene-d₂ crystals

Masaki Shimomura* and Masatoshi Iguchi

Research Institute for Polymers and Textiles, 1-1-4 Yatabe-Higashi, Tsukuba, Ibaraki 305, Japan

and Masamichi Kobayashi

Department of Macromolecular Science, Faculty of Science, Osaka University, Toyonaka, Osaka 560, Japan

(Received 21 May 1987; revised 9 July 1987; accepted 21 July 1987)

Infra-red and Raman spectra of two typical crystals of trigonal polyoxymethylene, i.e. needle-like crystals consisting of fully extended chains and solution-grown crystals of folded chains, are discussed in detail from a spectroscopic viewpoint. On going from needle-like to solution-grown crystals, some bands assigned to A₂ symmetry species shift towards the high-frequency side, while the other bands remain unshifted. Vibrational spectra of needle-like and solution-grown crystals of polyoxymethylene-d₂ are also measured and discussed.

(Keywords: trigonal polyoxymethylene; trigonal polyoxymethylene-d₂; vibrational spectra; needle-like crystal; solution-grown crystal)

INTRODUCTION

Polyoxymethylene (POM) is known as trigonal crystalline polymer consisting of chains basically of a 9/5 (or 29/16) helical conformation¹⁻³. Another modification, metastable orthorhombic POM crystal consisting of 2/1 helical chains, was first obtained by Mortillario *et al.* through polymerization of formaldehyde in aqueous solution⁴ and was recently found in a cationic polymerization system of trioxane⁵. Needle-like crystals of POM^{6,7} are known as trigonal single crystals having ultra-high perfection, consisting of extended 9/5 helical chains. Their highly ordered structure has been proved by X-ray diffraction, d.s.c. and other measurements⁸⁻¹⁰. Other typical trigonal single crystals are lamellar crystals, recrystallized from dilute solution, which consist of regularly folded molecular chains^{11,12}.

Vibrational spectra of POM have been of interest and a number of studies have been published. The assignment of the infra-red and Raman bands has by now been almost established with reference to theoretical normal-mode calculations¹³. It was reported first by Zamboni and Zerbi that the infra-red spectrum of POM changes with specimen treatment in the 1200-900 cm⁻¹ region¹⁴. Bands in this region were studied in detail by Oleinik and Enikolopyan by bringing in a series of oligomeric homologues¹⁵: it was assumed that the bands at 1238 and 903 cm⁻¹ were sensitive to the regular structure and were characteristic of a long *gauche* sequence, whereas 'additional' bands at 985 and 1130 cm⁻¹ were affiliated to a planar zig-zag conformation in the non-crystalline part. Terlemezyan *et al.* studied the structure of the specimen

obtained from cationic polymerization systems of trioxane in various solvents¹⁶⁻¹⁸. Infra-red spectra were classified into two types. It was concluded that these changes in the infra-red spectra were related to conformational defects in helical chains.

The infra-red spectral changes between needle-like and solution-grown crystals and other specimens of POM were investigated by Shimomura and Iguchi¹⁹. All of the infra-red bands of the needle-like crystals were assignable to the optically active fundamentals of the regular 9/5 helix of the POM molecule, and no additional bands appeared in the spectrum. For other POM specimens, on the contrary, the spectral pattern in the 1200-900 cm⁻¹ region exhibited substantial variation depending on the state and/or the route of processing of the samples. These remarkable spectral changes were thought to be related to some conformational defects in the crystalline part.

Fawcett proposed another interpretation of the changes in the infra-red spectra²⁰. These spectral changes were due to a difference in the chain packing, i.e. some molecules slide along the *c*-axis and intermolecular interactions were different as a result. Terlemezyan *et al.*²¹ argued against Fawcett's interpretation using a copolymer of trioxane and dioxolane in which slides along the *c*-axis exist. In spite of these works, interpretation of the difference in the infra-red spectra of trigonal POM is not clear.

In this article, infra-red and Raman spectra of trigonal POM crystals, especially two typical extremes, i.e. extended-chain needle-like crystals and folded-chain solution-grown single crystals of POM, are discussed in detail from a spectroscopic viewpoint. Vibrational spectra of the needle-like and solution-grown crystals of polyoxymethylene-d₂ (POM-d₂) are also measured and discussed.

* To whom correspondence should be addressed

EXPERIMENTAL

Samples

Needle-like crystals were prepared in a cationic polymerization system of trioxane under similar conditions as published previously⁷. Some samples were subjected to boron trifluoride etching⁸ to disrupt the original radial assembly.

Solution-grown crystals were prepared from the needle-like crystals, Delrin 500 or DuPont and other commercial acetal resins. Folded-chain crystals were recrystallized from dilute bromobenzene solution at various temperatures, typically from 0.5 wt % solution at 130°C. After filtration, crystals were freeze-dried using benzene. Since the needle-like crystals were insoluble in boiling bromobenzene, they had to be dissolved first in hexafluoroacetone sesquihydrate to destroy their highly crystalline structure and reprecipitated in acetone prior to the recrystallization from bromobenzene solution. Lamellar crystals grown from cyclohexanol solution were also examined.

Deuterated paraformaldehyde was used as the starting material of POM-d₂ synthesis. Trioxane-d₆ was prepared from deuterated paraformaldehyde and heavy water catalysed by silicotungstic acid. Needle-like crystals of POM-d₂ were prepared from trioxane-d₆ through the same procedures as in the case of the normal POM needle-like crystals. The boron trifluoride etching was not performed in this case. Solution-grown crystals of POM-d₂ were prepared from bromobenzene solution of the polymer obtained in the cationic polymerization system described above.

Infra-red absorption spectrum

A Jasco model 701G infra-red spectrometer was used. Sampling was performed by the Nujol mull method in order to avoid mechanical deformation, since by grinding with KBr powder, the solution-grown crystals transform very easily to another structure having different morphology, causing a significant spectral change. The recorded infra-red spectra were converted to absorbance scale and the background due to the mulling reagent was subtracted using a personal computer.

Far infra-red absorption spectrum

A Hitachi model FIS-3 far infra-red spectrometer was used. Powder samples were mixed with paraffin wax, spread on a silicon plate, and subjected to measurement.

Raman scattering spectrum

Powder samples were sealed in glass ampoules and Raman spectra were measured with a Jasco model R-500 double monochromator using the 514.5 nm line from an Ar⁺ laser as the excitation source.

X-ray diffraction measurement

A Philips model PW1700 system with a graphite monochromator was used. Data were also processed using the personal computer.

RESULTS AND DISCUSSION

In ref. 19, it was found that the infra-red spectrum of the needle-like crystals was in good accord with the results of the normal-mode calculations, while some bands of the

solution-grown crystals shifted substantially from the positions of the corresponding bands of the needle-like crystals. Rather complicated spectral profiles of other trigonal POM specimens could be explained as the overlap of these two extreme spectra. In *Figure 1*, the infra-red spectra (1300–400 cm⁻¹ region) of trigonal POM in the two extreme crystalline morphologies, i.e. the extended-chain (needle-like) crystals (ECC) and the folded-chain (solution-grown) crystals (FCC), are compared with each other. Since the solution-grown crystals are very easy to change by mechanical deformation during pelletization into KBr pellet, the Nujol mull method was adopted in this study.

The difference in spectra between the two cases is quite obvious. In the solution-grown crystals, the 1093 and 895 cm⁻¹ bands of the needle-like crystals almost disappear and, instead, new bands appear at 1138 and 1000 cm⁻¹. The other bands are common in both samples. Solution-grown crystals recrystallized from the needle-like crystals and other commercial acetal resins give almost the same infra-red spectra as that shown in *Figure 1* (lower). The spectrum of the solution-grown crystals recrystallized from cyclohexanol solution is also the same as those of the other solution-grown crystals. From these facts, it is evident that the spectral difference between the needle-like and solution-grown crystals can be ascribed not to a difference in chemical structure but to a difference in morphological structure. The same comparison has been made also for the far infra-red region (*Figure 2*). The difference is also clear. The band at 220 cm⁻¹ of the needle-like crystals shifts to 234 cm⁻¹ in the solution-grown crystals. The weak bands around 300 cm⁻¹ in the needle-like crystals are due to the small amount of orthorhombic form contained (a few mol%).

Raman spectra of these two samples are reproduced in *Figure 3*. In contrast to the infra-red spectra, no significant difference is found as far as the peak positions are concerned.

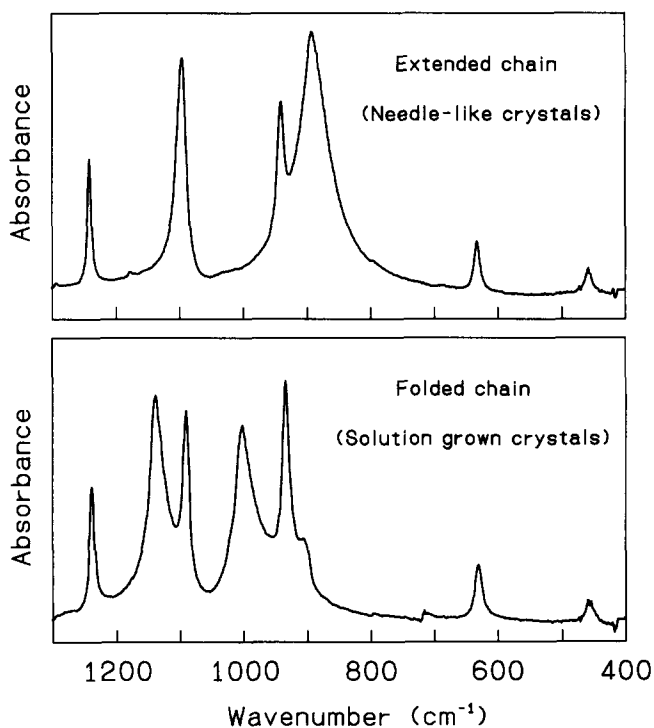


Figure 1 Infra-red spectra of polyoxymethylene crystals

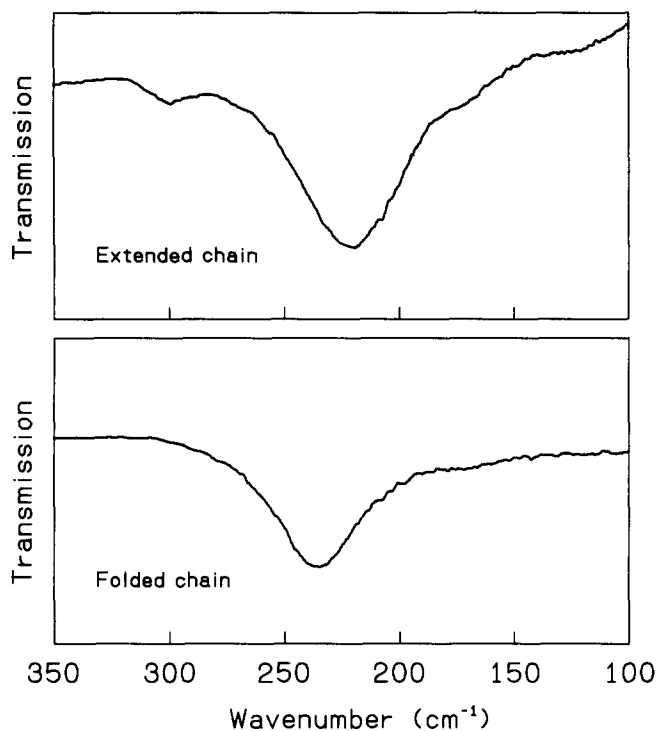


Figure 2 Far infra-red spectra of polyoxymethylene crystals

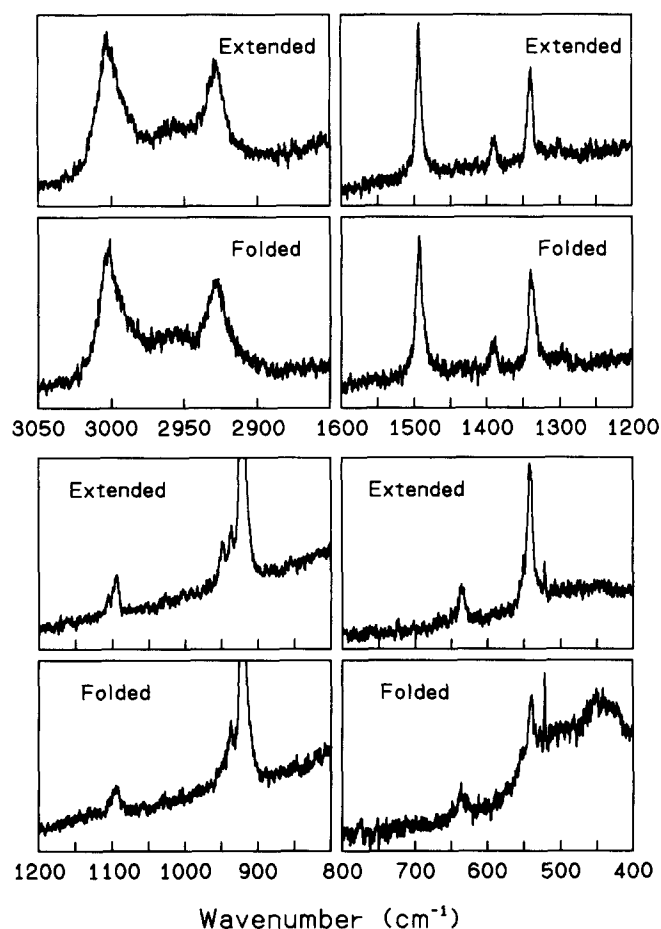


Figure 3 Raman spectra of polyoxymethylene crystals

Figure 4 shows the wide-angle X-ray diffraction patterns of these two crystals. The sharpness of the X-ray diffraction peaks of the needle-like crystals proves the very high crystalline perfection. The crystallinity of the

solution-grown crystals is also nearly as high as for polymer crystals, as is recognized from the small background scattering due to the amorphous part. Although the sharpness of the peaks is not the same, the reflections of the two crystals are basically identical. This means that as far as the unit-cell structure is concerned these two crystals are of the same trigonal phase consisting of 9/5 helices.

The optically active (or the zone-centre) molecular vibrations of the 9/5 helix are classified into A_1 , A_2 , E_1 , E_2 , E_3 and E_4 species, where the A_2 and E_1 modes are infra-red-active, the A_1 , E_1 and E_2 modes are Raman-active and the E_3 and E_4 are inactive in both infra-red and Raman spectra. The vibrational spectra of the needle-like crystals are readily assignable in accordance with the established normal-mode calculations¹³, which have been based on spectral data measured on highly crystalline and highly oriented POM resins. In Table 1, the observed wavenumbers of the infra-red absorption bands and the corresponding calculated frequencies of the A_2 and E_1 species are summarized. The observed and calculated frequencies of the Raman-active A_1 and E_1 modes are also listed (E_2 modes are omitted here). No significant difference is found between the A_1 and E_1 bands of the two samples. Previously, complementary relationships of the intensities for the 1138 and 1093 cm^{-1} band pair and the 1000 and 895 cm^{-1} band pair in the infra-red spectra have been found among various POM specimens different in origin as well as in prehistory¹⁹. From this fact and the results given in Table 1, the infra-red spectral changes of trigonal POM might be explained as follows. The 895 and 220 cm^{-1} bands and one of the overlapping components around 1093 cm^{-1} of the needle-like crystals shift, respectively, to 1000, 234 and 1138 cm^{-1} in the solution-grown crystals; on going from the needle-like to the solution-grown crystals, some of the A_2 bands shift towards the high-frequency side, while the

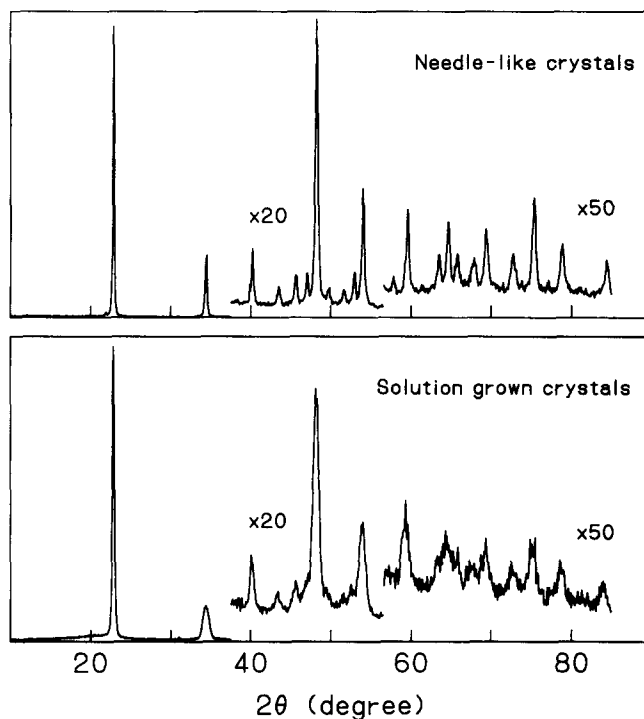


Figure 4 X-ray diffraction diagrams of polyoxymethylene crystals

Table 1 Vibrational bands of polyoxymethylene

| Species | Calculated ¹³ (cm ⁻¹) | Observed (cm ⁻¹) | | | |
|----------------|---|------------------------------|----------------|-------------|----------------|
| | | Infra-red | | Raman | |
| | | Needle-like | Solution-grown | Needle-like | Solution-grown |
| A ₁ | 2924 | Inactive | | 2928 s | 2928 s |
| | 1508 | | | 1493 s | 1493 s |
| | 1330 | | | 1339 m | 1339 m |
| | 916 | | | 921 vs | 922 vs |
| | 587 | | | 542 m | 540 w |
| A ₂ | 2977 | 2985 m | 2983 m | Inactive | |
| | 1425 | 1385 vw | 1385 vw | | |
| | — | — | 1138 s | | |
| | 1118 | 1093 s | — | | |
| | — | — | 1000 s | | |
| | 922 | 895 vs | 905 vw | | |
| | — | — | 234 | | |
| 237 | 220 | — | | | |
| E ₁ | 2982 | 2999 w | 2998 w | 3003 s | 3003 s |
| | 2926 | 2928 m | 2926 m | — | — |
| | 1506 | 1470 vw | 1470 vw | — | — |
| | 1407 | 1435 vw | 1435 vw | — | — |
| | 1318 | — | — | 1300 w | 1298 vw |
| | 1169 | 1240 m | 1240 m | — | — |
| | 1072 | 1093 s | 1093 m | 1095 m | 1095 m |
| | 930 | 938 m | 935 m | 937 w | 937 w |
| | 634 | 633 w | 633 w | 636 w | 636 w |
| | 483 | 457 | 460 | — | — |
| | 22 | — | — | — | — |

other bands remain unshifted. The symmetry species of the infra-red bands of the needle-like crystals have been determined by polarization measured on highly oriented film specimens. In contrast, the above-mentioned infra-red bands characteristic of solution-grown crystals remain unassigned because of the lack of polarization data.

To check the species of the unassigned, shifted bands of the solution-grown crystals, infra-red spectra of random and plane-oriented solution-grown crystals were measured. The latter sample was prepared by pressing a powder of the solution-grown crystals between two KBr windows with a small amount of liquid paraffin. In this process, the plate-shaped crystals are partly oriented with *c*-axis directed normal to the window surface (a plane orientation). On measuring the transmission spectrum of this sample, the incident infra-red radiation is nearly parallel to the *c*-axis, so that the *c*-polarized A₂ bands should diminish compared with the spectrum taken on a randomly oriented powder sample. The degree of plane orientation decreases with increasing thickness of mulled powder between the windows. By insertion of a spacer of sufficient thickness, we are able to prepare randomly oriented solution-grown crystals.

Figure 5 shows the infra-red spectra of the solution-grown crystals in a random and a semi-plane orientation. The absorption bands of the semi-oriented sample at 1138 and 1000 cm⁻¹ are much weaker than those of the random sample compared with the other five E₁ bands. This means that the unassigned bands at 1138 and 1000 cm⁻¹ should be classified to the A₂ mode. This result also supports the hypothesis that the difference in the infra-red spectrum among various trigonal POM samples is caused by significant frequency shifts of some

of the A₂ bands on changing the morphology between the ECC and the FCC types.

In order to get other spectral evidence, deuterated POM samples were synthesized and their vibrational spectra were examined. During the synthesis of the needle-like crystals, an orthorhombic modification was sometimes generated as a by-product²². Though the X-ray diffraction pattern of the needle-like crystals of POM-d₂ indicates contamination of a few per cent of the orthorhombic form, it does not interfere with the analysis of the vibrational spectra.

Figure 6 shows the infra-red spectra of POM-d₂. As expected, a remarkable difference is found between the two crystals. Although the spectra are more complicated than those of normal POM, the bands of the needle-like crystals are readily assignable with reference to the literature¹³. The far infra-red spectra of both samples were also measured (Figure 7). Here the difference is rather simple, that is, the band at 365 cm⁻¹ is common and the 199 cm⁻¹ band of the needle-like crystals shifts to 214 cm⁻¹ in the solution-grown crystal. Figure 8 shows the Raman spectra of POM-d₂. Like normal POM, the bands of the two crystals appear at the same positions.

The observed frequencies of the infra-red bands and the corresponding calculated values are listed in Table 2. The Raman bands of POM-d₂ are also listed (E₂ modes are omitted). The bands assigned to the A₂ modes, at 958, 830 and 199 cm⁻¹ of the needle-like crystals, almost disappear in the solution-grown crystals and new bands appear at 1095, 850 and 214 cm⁻¹. In contrast, the bands of the A₁ and E₁ modes appear at the same positions.

Figure 9 shows the infra-red spectra of random and plane-oriented solution-grown crystals of POM-d₂. The bands at 1095 and 850 cm⁻¹ diminish remarkably in the semi-oriented sample and are assigned to the A₂ species. There is an unassigned band at 969 cm⁻¹ in both crystals.

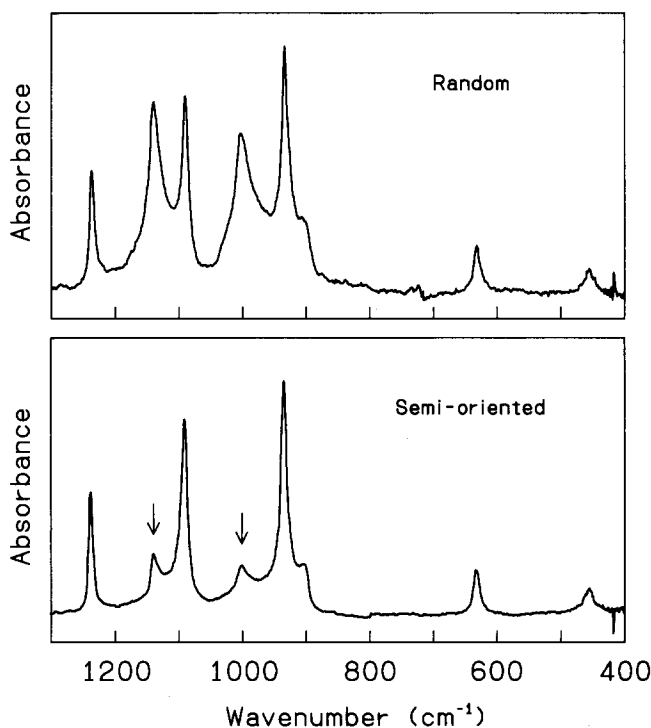
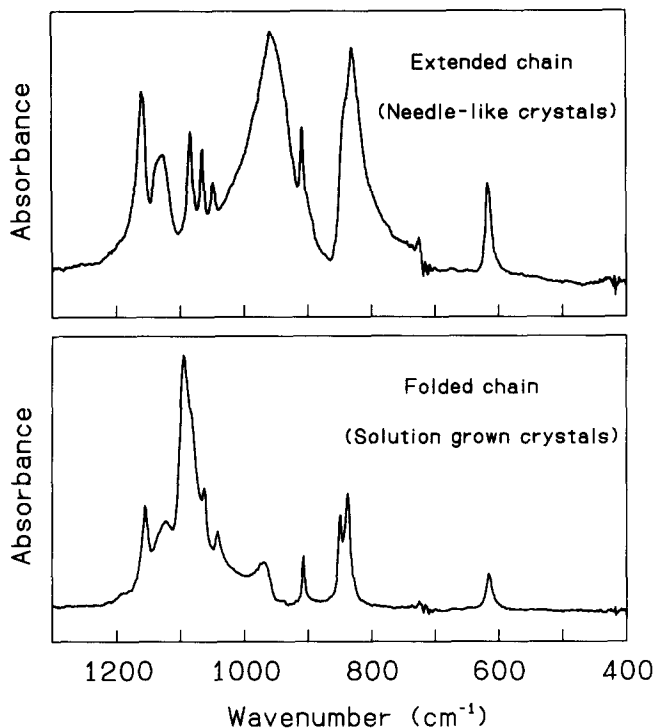
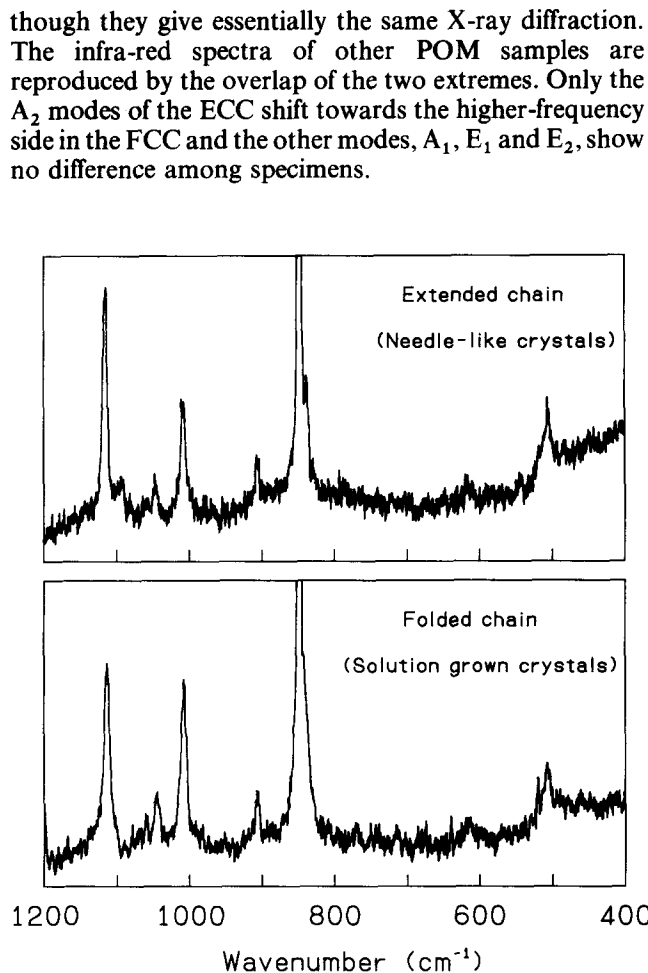
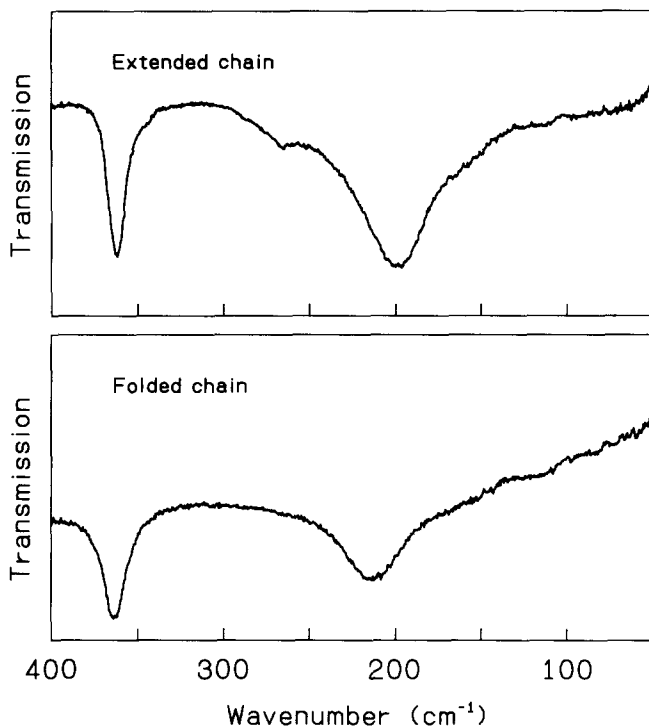


Figure 5 Infra-red spectra of random and plane-oriented solution-grown crystals of polyoxymethylene


 Figure 6 Infra-red spectra of polyoxymethylene-d₂ crystals

 Figure 8 Raman spectra of polyoxymethylene-d₂ crystals

 Figure 7 Far infra-red spectra of polyoxymethylene-d₂ crystals

This band may be due to the amorphous or folding part. Because of overlapping, weak bands at around 1048–1042 cm⁻¹ cannot be assigned. Thus, we conclude that the A₂ bands of the POM-d₂ needle-like crystals (958, 830 and 199 cm⁻¹) shift to 1095, 850 and 214 cm⁻¹, respectively, in the spectra of the solution-grown crystals.

From these results, the changes in the vibrational spectra of trigonal POM, and POM-d₂ as well, are summarized as follows. Two extreme crystals, the ECC and the FCC, give quite different infra-red spectra,

though they give essentially the same X-ray diffraction. The infra-red spectra of other POM samples are reproduced by the overlap of the two extremes. Only the A₂ modes of the ECC shift towards the higher-frequency side in the FCC and the other modes, A₁, E₁ and E₂, show no difference among specimens.

 Table 2 Vibrational bands of polyoxymethylene-d₂

| Species | Calculated ^{1,3} (cm ⁻¹) | Observed (cm ⁻¹) | | | |
|----------------|--|------------------------------|----------------|-------------|----------------|
| | | Infra-red | | Raman | |
| | | Needle-like | Solution-grown | Needle-like | Solution-grown |
| A ₁ | 2121 | Inactive | | | |
| | 1126 | | | 1115 s | 1114 s |
| | 1013 | | | 1009 m | 1008 s |
| | 828 | | | 850 vs | 850 vs |
| | 557 | | | 506 m | 507 w |
| A ₂ | 2193 | | | Inactive | |
| | — | | 1095 vs | | |
| | 1154 | 1048 w | 1042 w | | |
| | — | | 969 m | | |
| | 1026 | 958 vs | | | |
| | — | | 850 m | | |
| | 769 | 830 vs | | | |
| — | | 214 | | | |
| 212 | 199 | | | | |
| E ₁ | 2207 | | | | |
| | 2121 | | | | |
| | 1178 | 1159 s | 1156 m | | |
| | 1145 | 1127 m | 1124 m | | |
| | 1047 | 1083 m | 1083 sh | | |
| | 1044 | 1065 m | 1063 m | | |
| | 916 | 908 m | 907 m | 907 w | 907 m |
| | 810 | 840 sh | 839 s | 838 w | — sh |
| | 618 | 617 m | 616 m | 617 vvw | 616 vvw |
| | 372 | 365 | 364 | | |
| 21 | | | | | |

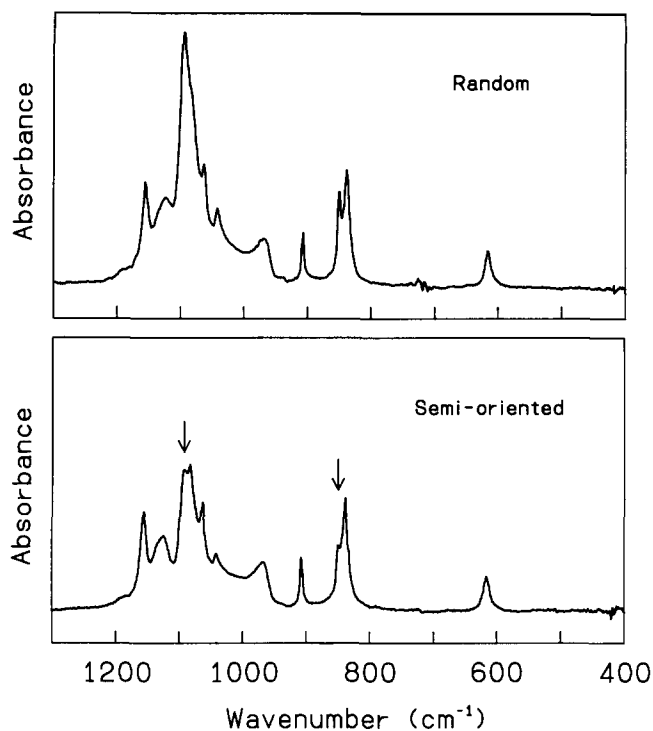


Figure 9 Infra-red spectra of random and plane-oriented solution-grown crystals of polyoxymethylene-d₂

In considering the origin of the specific infra-red spectrum of the FCC, possibility of another crystal modification other than the previously known trigonal and orthorhombic forms must be checked first. The X-ray diffraction pattern and the Raman spectrum of the solution-grown crystals are of the typical trigonal form.

Fawcett proposed a model of structural inhomogeneities in trigonal POM²⁰, where some chains in the lattice advanced by half of the pitch of the repeat unit along the *c*-axis. He supposed that the difference in intermolecular interactions caused the changes in the infra-red spectrum. Terlemezyan and Mihailov denied this possibility using trioxane-dioxolane copolymer²¹.

Solution-grown crystals of ethylene oxide copolymer and tetramethylene oxide copolymer were also examined by the present authors. In the infra-red spectra of the FCC of the copolymers, the bands at 1138 and 1000 cm⁻¹ were observed and only a shoulder was found at about 900 cm⁻¹. These results mean that Fawcett's interpretation of the spectral change is not appropriate. Also, conformational defects in the (CH₂)₂ or (CH₂)₄ unit cannot make the shifts of the A₂ modes.

Oleinik and Enikolopyan¹⁵ thought that the bands at 1138 and 1000 cm⁻¹ were due to defects such as planar zig-zag conformations in non-crystalline parts. Because of its high crystallinity and low amount of non-crystalline part, this cannot explain the shift in the FCC.

Terlemezyan *et al.*¹⁸ explained the bands as follows. The bands at 1128 and 988 cm⁻¹ arise from short regular *gauche* conformations, in other words, from a high content of conformational defects such as *trans* form in helix. The band at 900 cm⁻¹ was related to long regular *gauche* conformations. Such defects might change the selection rules and the appearance of new bands might be expected, but the disappearance of the 900 cm⁻¹ band and the diminishing of the 1093 cm⁻¹ band could not be explained. From the other point of view, fewer defects

would exist in the solution-grown crystals than in melt-crystallized film, since the solution-grown crystals were prepared by isothermal crystallization from dilute solution and were expected to have better perfection than the melt film. Experimentally, the melt-crystallized film and other defective specimens showed stronger absorption bands at 1093 and 900 cm⁻¹. Thus the spectral change among various POM specimens could not be interpreted by conformational defects such as planar zig-zag forms in the crystalline part. The shifts of the A₂ bands are due to some uniform structural difference in the crystalline part of the ECC and the FCC.

By the normal-mode calculations, a small difference of helical pitch (or conformation), which is not detected by X-ray diffraction, cannot make such large shifts (up to about 100 cm⁻¹) of the A₂ modes but have to cause small shifts for all species to both higher- and lower-frequency sides. Such differences cannot explain the spectral change of the FCC trigonal POM.

Another possibility of spectral change, namely splitting of bands, should be considered. The extent of the frequency shifts of trigonal-form POM are much larger than those of splittings due to interchain interactions observed in the orthorhombic form. All three A₂ bands shifted to the higher-frequency region and no bands appeared in the lower region in the spectrum of the FCC. From these facts, it is difficult to interpret the spectral change as the splitting of the A₂ bands. The next possibility was a mixing with modes of other species. If mixing of modes did occur in the FCC, some A₁ bands should appear in the infra-red spectrum and A₂ bands should be found in the Raman spectrum. However, in the vibrational spectra of the FCC, the selection rule is kept and mixing of modes does not occur.

CONCLUSIONS

The changes in the vibrational spectra of POM and POM-d₂ are very interesting phenomena. The needle-like and solution-grown crystals, which give the same X-ray diffraction patterns, show quite different vibrational spectra. In the spectra of the FCC, only the bands assigned to the A₂ modes shift to the higher frequency and all bands of other species, A₁ and E₁, are the same as those of the ECC. The spectra of the POM specimens between the two extremes could be reproduced as the overlap of the two spectra.

Thus no interpretation can be made from the viewpoint of vibrational spectroscopy. A new concept, e.g. an interaction between induced dipole moments, might be necessary to explain the spectral changes of trigonal POM and POM-d₂.

REFERENCES

- 1 Tadokoro, H., Yasumoto, S., Murahashi, S. and Nitta, I. *J. Polym. Sci.* 1960, **44**, 266
- 2 Uchida, T. and Tadokoro, H. *J. Polym. Sci. (A-2)* 1967, **5**, 63
- 3 Carazzolo, G. *J. Polym. Sci. (A)* 1963, **1**, 1573
- 4 Mortillario, L., Galliazzo, G. and Bessi, S. *Chem. Ind. (Milan)* 1964, **46**, 139, 144
- 5 Iguchi, M. *Polymer* 1983, **24**, 915
- 6 Iguchi, M. *Br. Polym. J.* 1973, **5**, 195
- 7 Iguchi, M. and Murase, I. *J. Crystal Growth* 1974, **24/25**, 596
- 8 Iguchi, M., Murase, I. and Watanabe, K. *Br. Polym. J.* 1974, **6**, 61
- 9 Iguchi, M. *Makromol. Chem.* 1976, **177**, 549

- | | |
|---|--|
| <p>10 Mashimoto, T., Sakai, T. and Iguchi, M. <i>J. Phys. (D)</i> 1979, 12, 1567</p> <p>11 Bassett, D. C., Dammont, F. R. and Salovey, R. <i>Polymer</i> 1964, 5, 579</p> <p>12 Carter, D. R. and Baer, E. <i>J. Appl. Phys.</i> 1966, 37, 4060</p> <p>13 Tadokoro, H., Kobayashi, M., Kawaguchi, Y., Kobayashi, A. and Murahashi, S. <i>J. Chem. Phys.</i> 1963, 38, 703</p> <p>14 Zamboni, V. and Zerbi, G. <i>J. Polym. Sci. (C)</i> 1964, 7, 153</p> <p>15 Oleinik, E. F. and Enikolopyan, N. S. <i>J. Polym. Sci. (C)</i> 1968, 16, 3677</p> | <p>16 Terlemezyan, L., Mihailov, M., Schmidt, P. and Schneider, B. <i>Makromol. Chem.</i> 1978, 179, 807</p> <p>17 Terlemezyan, L., Mihailov, M., Schmidt, P. and Schneider, B. <i>Makromol. Chem.</i> 1978, 179, 2315</p> <p>18 Terlemezyan, L. and Mihailov, M. <i>Eur. Polym. J.</i> 1981, 17, 1115</p> <p>19 Shimomura, M. and Iguchi, M. <i>Polymer</i> 1982, 23, 509</p> <p>20 Fawcett, A. H. <i>Polym. Commun.</i> 1982, 23, 1865</p> <p>21 Terlemezyan, L. and Mihailov, M. <i>Polym. Commun.</i> 1984, 25, 80</p> <p>22 Kobayashi, K., Itoh, Y., Tadokoro, H., Shimomura, M. and Iguchi, M. <i>Polym. Commun.</i> 1983, 24, 38</p> |
|---|--|